INL/RPT-24-80341

Advanced Reactor Technologies

# Pre-Test Feasibility Study Of Reactivity Transient Testing On TRISO Fuel In The TREAT Reactor

M3TG-24IN0402071

SEPTEMBER 2024

Jacob A. Hirschhorn,
Mustafa K. Jaradat,
Ryan T. Sweet,
Paul A. Demkowicz,
Paolo Balestra, and
Gerhard Strydom

*Idaho National Laboratory*

Idaho National Laboratory

INL/RPT-24-80341

# Pre-Test Feasibility Study Of Reactivity Transient Testing On TRISO Fuel In The TREAT Reactor

M3TG-24IN0402071

Jacob A. Hirschhorn,
Mustafa K. Jaradat,
Ryan T. Sweet,
Paul A. Demkowicz,
Paolo Balestra, and
Gerhard Strydom
Idaho National Laboratory

September 2024

Idaho National Laboratory
INL ART Program
Idaho Falls, Idaho 83415

http://www.inl.gov

Prepared for the
U.S. Department of Energy
Office of Nuclear Energy
Under DOE Idaho Operations Office
Contract DE-AC07-05ID14517

*Page intentionally left blank*

**INL ART Program**

# Pre-Test Feasibility Study of Reactivity Transient Testing on TRISO Fuel in the TREAT Reactor

**INL/RPT-24-80341**

**September 2024**

**Technical Reviewer:** (Confirmation of mathematical accuracy, and correctness of data and appropriateness of assumptions.)

| | |
|---|---|
| David Alan Reger<br>Nuclear Engineer | Date |

**Approved by:**

| | |
|---|---|
| Michael E. Davenport<br>ART Project Manager | Date |
| Travis R. Mitchell<br>ART Program Manager | Date |
| Michelle T. Sharp<br>INL Quality Assurance | Date |
| Name<br>Title | Date |

*Page intentionally left blank*

ABSTRACT

Uranium oxycarbide (UCO)-bearing tri-structural isotropic (TRISO) particle fuels are expected to be used in numerous U.S. commercial reactor applications within the next decade. In this work, we reviewed historical particle fuel transient experiments to identify gaps in TRISO fuel performance transient testing. A BISON–Griffin modeling framework was then developed to conduct preliminary TRISO transient analyses and begin to address these gaps. The framework was demonstrated using limiting-case transient conditions from a prototypic high-temperature gas-cooled reactor (HTGR). It was then applied to develop a matrix of experiments that could be performed in the Transient Reactor Test Facility (TREAT) to (1) evaluate UCO-fueled particle performance at moderate and high heat rates, (2) assess whether historical testing involving $UO_2$-fueled particles is applicable to modern UCO-fueled particles, (3) deconvolute the impacts of temperature and heat rate on particle transient response, and (4) collect the data needed for fuel performance model validation and/or further development.

*Page intentionally left blank*

# CONTENTS

# FIGURES

# TABLES

*Page intentionally left blank*

# ACRONYMS

| | |
|---|---|
| AGR | Advanced Gas Reactor |
| ARDP | Advanced Reactor Demonstration Program |
| ATR | Advanced Test Reactor |
| AVR | Arbeitsgemeinschaft Versuchsreaktor |
| BAF | Bacon anisotropy factor |
| CRW | control rod withdrawal |
| CZP | cold-zero power |
| DBA | design basis accident |
| FGR | fission gas release |
| FHR | fluoride-salt-cooled high-temperature reactor |
| HTGR | high-temperature gas-cooled reactor |
| HTR-10 | High Temperature Gas-cooled Reactor Test Module |
| HTTR | High Temperature Engineering Test Reactor |
| IGR | Impulse Graphite Reactor |
| IIDC | irradiation-induced dimensional change |
| IPyC | inner pyrolytic carbon |
| LWR | light water reactor |
| MOOSE | Multiphysics Object-Oriented Simulation Environment |
| NDMAS | Nuclear Data Management and Analysis System |
| NSRR | Nuclear Safety Research Reactor |

| | |
|---|---|
| NTP | nuclear thermal propulsion |
| OPyC | outer pyrolytic carbon |
| PyC | pyrolytic carbon |
| SiC | silicon carbide |
| TREAT | Transient Reactor Test Facility |
| TRISO | tri-structural isotropic |
| UCO | uranium oxycarbide |

*Page intentionally left blank*

# Pre-Test Feasibility Study of Reactivity Transient Testing on TRISO Fuel in the TREAT Reactor

### M3TG-24IN0402071

## 1. INTRODUCTION

Particle-based fuels are slated for use in numerous U.S. commercial reactor applications expected to be deployed within the next decade. Particle-based fuels generally consist of multi-layer encapsulated fuel particles arranged within a graphite, silicon carbide (SiC), or other carbonaceous matrix to form pebbles or compacts. The applications mentioned above are likely to utilize particles similar to the uranium oxycarbide (UCO)-fueled tri-structural isotropic (TRISO) design developed under the U.S. Advanced Gas Reactor (AGR) Program [1].

This particle design consists of a UCO kernel surrounded by a low-density carbon buffer layer, which provides free volume to accommodate fission gases released from the kernel and mechanical deformation of neighboring layers [2]. This is covered by an inner pyrolytic carbon (IPyC) layer, which contributes to retention of non-metallic fission products and provides support for the SiC layer that follows. The SiC layer is primarily responsible for retention of metallic fission products and acts as the primary pressure vessel for the fuel form. The final particle layer is the outer pyrolytic carbon (OPyC), which serves a purpose similar to that of the IPyC and additionally protects the SiC during particle overcoating and compaction processes.

The U.S. Nuclear Regulatory Commission provides guidance for the design and operation of nuclear power plants in the Code of Federal Regulations and various technical and topical reports. This guidance is used to develop functional requirements, operational requirements, and fuel design criteria for specific engineering applications. Among other things, these requirements establish metrics for containment of radioactive nuclides. These metrics must be satisfied during both steady-state (normal) and transient operation, which includes various anticipated operational occurrences, design basis accidents (DBAs), and beyond design basis accidents relevant to each reactor type.

Because radionuclides can be released from both intact and failed particles, release calculations must account for the amount of radioactivity released from each particle type, as well as the probability of particle failure. A particle is typically considered to have failed when its SiC layer has been mechanically and/or chemically compromised. Fuel performance codes have been developed to model these behaviors and the irradiation, thermomechanical, and thermochemical processes on which they depend [3]. These codes can be applied throughout the fuel development life cycle—from scoping calculations used to identify promising designs, to confirmatory analyses used to support qualification and licensing.

One such code is BISON, a finite element-based fuel performance code developed by numerous U.S. institutions and maintained by Idaho National Laboratory [4]. BISON, which is based on the Multiphysics Object-Oriented Simulation Environment (MOOSE) Framework [5], features a multitude of TRISO modeling capabilities [6] and has been applied extensively to conduct TRISO fuel performance and failure calculations [7]. Combining BISON with codes like Griffin, a MOOSE-based reactor multiphysics application [8, 9], yields a formidable toolkit for TRISO source term analysis and experiment design.

The purpose of this work is to identify gaps in the TRISO transient fuel performance design space and demonstrate a multiphysics analysis framework based on BISON and Griffin, which could be applied to help design and interpret targeted experiments to fill those gaps. We begin by briefly reviewing the history of particle fuel transient testing and analysis. Guided by publicly-available information about the U.S. commercial reactor applications expected to utilize TRISO fuels, we then define a preliminary transient fuel performance design space and identify potential gaps in our current understanding. Next, we apply a new multiphysics analysis framework based on BISON and Griffin to conduct preliminary TRISO fuel

performance analyses using limiting-case transient conditions from a prototypic high-temperature gas-cooled reactor (HTGR).

Finally, we identify a series of targeted Transient Reactor Test Facility (TREAT) experiments intended to address gaps in the design space and apply the codes to demonstrate how they can be leveraged to aid in experiment design and interpretation of experimental data. Ultimately, this work is intended to support deployment of TRISO fuels for commercial U.S. applications by identifying opportunities to improve our understanding of TRISO fuel performance and providing a concrete demonstration of how existing codes and experimental facilities can be effectively utilized to design and conduct relevant experiments.

# 2. HISTORY OF PARTICLE FUEL TRANSIENT ANALYSIS

Several in-depth reviews of TRISO in-pile steady-state testing, out-of-pile high-temperature testing, and fuel performance modeling are available in the open literature [2, 3]. This work focuses on in-pile transient testing, for which an excellent review was recently published by Brown [10]. An in-depth examination of the material covered by Brown is beyond the scope of this work. Instead, we examine major trends and advancements in the study of TRISO performance during transients within the context of ongoing commercialization efforts. A timeline of these events is shown in Figure 1.

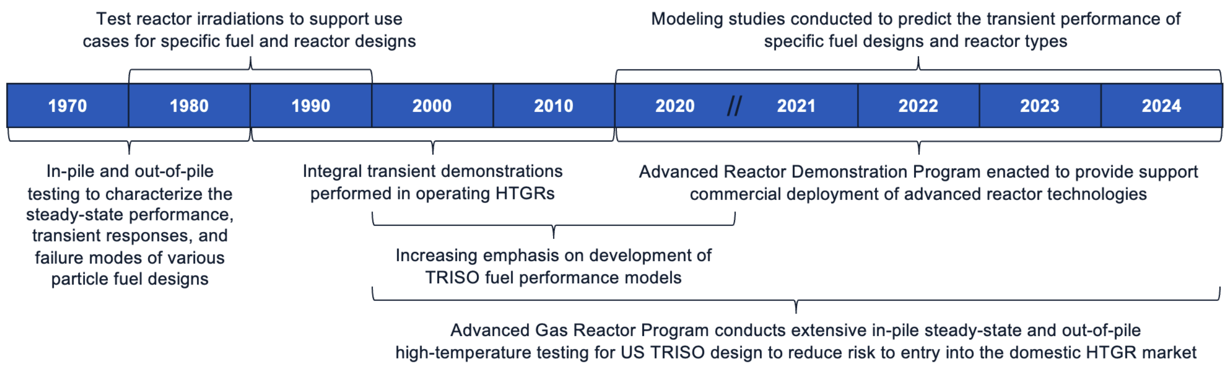


Figure 1. Simplified timeline highlighting major trends and advancements relevant to the study of TRISO performance during transient operations. Early experiments were conducted with numerous types of particle fuels to identify promising designs and characterize their failure behaviors, paving the way for focused transient experiments in test reactors, and ultimately, operating HTGRs. These and other steady-state data were used to develop TRISO fuel performance models, which have since been applied to predict TRISO performance under various HTGR and non-HTGR operating conditions. These models have been leveraged extensively by the U.S. AGR program and to support commercial deployment of TRISO-fueled advanced reactors as part of the Advanced Reactor Demonstration Program (ARDP) and other public and private activities.

Early experiments subjected numerous types of particle fuels to in-pile and out-of-pile testing to identify promising designs and characterize their failure behaviors [11]. Design variables included fuel material (e.g., $UC_2$, $ThO_2$, and $UO_2$), layer structure (e.g., bi-structural isotropic and TRISO), layer dimensions, and fabrication techniques. Particle failure behaviors including kernel migration, over-pressurization, and Pd penetration were characterized over a range of operating conditions. They identified promising designs and concluded that particles fabricated within specifications are not likely to fail under prototypic HTGR conditions. Observed particle failures were attributed to fabrication defects and/or exposure to abnormally high temperatures in *thermal excursion tests* designed to simulate transient operations.

Those early studies paved the way for more focused transient experiments in test reactors such as the

Nuclear Safety Research Reactor (NSRR), HYDRA, and the Impulse Graphite Reactor (IGR) [12–14]. The NSRR and HYDRA tests subjected both loose particles and compacts to pulsed irradiations with energy depositions ranging from 100-2300 J/g-fuel and pulse widths of 1-5 ms. Evidence of fuel melting was noted in several tests, and particle and matrix failure was correlated to energy deposition. The IGR tests subjected compacts to energy depositions in excess of 10,000 J/g-fuel using significantly longer pulses to characterize matrix failure behaviors. All of the above tests were conducted with $UO_2$-fueled particles.

Subsequent transient testing was performed in operating HTGRs, including the Arbeitsgemeinschaft Versuchsreaktor (AVR), High Temperature Gas-cooled Reactor Test Module (HTR-10), and High Temperature Engineering Test Reactor (HTTR) [15–19]. Tests were conducted with both pebbles and prismatic compacts bearing $UO_2$-fueled particles. The experiments successfully demonstrated that acceptable fuel performance could be maintained during prototypic pressurized loss of forced convection, depressurized loss of forced convection, and control rod withdrawal (CRW) transients.

Data from the preceding tests and other steady-state testing were used to develop TRISO fuel performance models [3]. These have since been applied to model TRISO fuel performance in the aforementioned test reactor irradiations [20, 21] as well as under prototypic HTGR [22–24], fluoride-salt-cooled high-temperature reactor (FHR) [25, 26], and light water reactor (LWR) [27] transients. The models have also been used extensively by the AGR program to model TRISO fuel performance during steady-state irradiations [1, 28–30] and out-of-pile safety tests [31, 32] in support of its mission to reduce risk of entry into the commercial U.S. HTGR market.

Demand for these data and tools increased dramatically in the 2020s with the beginning of the U.S. ARDP. The program, along with other public and private activities, is intended to support commercial deployment of advanced reactor technologies in the U.S., including those fueled by TRISO. Currently, plans are in place to develop TRISO-fueled reactors based on HTGR, FHR, LWR, and heat pipe technologies within the next decade. Acceleration of these commercialization efforts make this the ideal time to assess the remaining gaps in the transient TRISO fuel performance design space.

# 3. TRANSIENT GAP ANALYSIS

Early scoping studies established the general behavior of various particle fuels. Subsequent test reactor irradiations improved confidence in their use by beginning to characterize the failure envelope of $UO_2$-fueled particles under transient conditions. These studies correlated failure to the total energy deposited in particles over the course of very short pulse irradiations.

While total energy deposition and pulse width are reasonable metrics for describing test reactor irradiations, they are less useful for correlating fuel performance behaviors to the conditions present in commercial power reactors during transient operation. Metrics such as transient initiation temperature and characteristic heat rate may be more useful. The transient temperature is important because it directly impacts nearly all thermomechanical and thermochemical material properties. The characteristic heat rate, or rate of change of temperature, is important due to its potential impact on temperature-dependent phenomena that occur over different time scales.

One example of a transient phenomenon is differential thermal expansion of TRISO layers at a rate that exceeds the ability of creep to relieve the resulting stresses, which could increase the likelihood of layer fracture and/or debonding. This phenomenon highlights a potentially impactful difference between in-pile and out-of-pile testing. In-pile testing, where heat is produced in the kernel and migrates outward through the coating layers, produces distinctly different temperature gradients (and therefore deformation behaviors and stresses) than out-of-pile testing, where heat is supplied by a furnace and migrates into the particle. Differences in how particles perform under these different testing conditions are not thoroughly understood. Another example is fission gas bubble over-pressurization and micro-cracking, which is associated with transient fission gas release (FGR) in ceramic fuels used in LWR applications [33]. This phenomenon, which

is sometimes referred to as “burst release” and cannot be attributed to typical diffusive release mechanisms, could potentially increase particle internal pressure and therefore layer stresses.

Unfortunately, the large deposited energies, narrow pulse widths, and general setups of the test reactor irradiations (which frequently induced fuel melting) make it difficult to determine accurate thermal histories for the samples. This, in turn, makes it difficult to correlate the observed behaviors to the power and cooling conditions that may be present during realistic transients in commercial power reactors. Data from subsequent transient testing in AVR, HTR-10, and HTTR are more readily applicable, but still limited to $UO_2$-fueled particles in HTGRs.

Finally, the AGR program successfully demonstrated acceptable performance for UCO-fueled particles in a series of in-pile steady-state and out-of-pile safety tests. The AGR experiments and the historical tests discussed above are arranged within a qualitative parameter space defined by transient temperature and characteristic heat rate in Figure 2. The types of TRISO-fueled reactors being considered for near-term commercial deployment and the adequacy of the coverage in various regions of the parameter space are used to identify specific gaps in our transient understanding below.

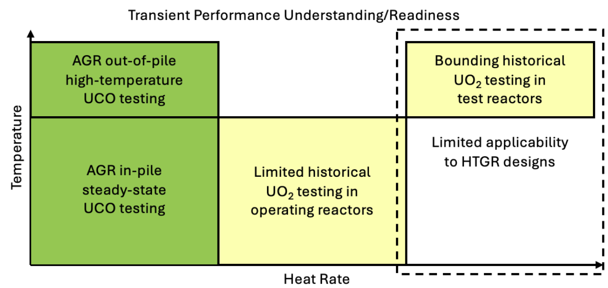


Figure 2. Qualitative diagram illustrating where historical and AGR program experiments fall within the transient parameter space defined by transient temperature and characteristic heat rate. The diagram highlights regions of the HTGR and non-HTGR parameter spaces that have not yet been explored. These observations form the basis of the preliminary gap analysis conducted in the current work.

The authors emphasize that TRISO fuels have exhibited outstanding levels of safety and predictability for HTGRs under normal operation and accident conditions. The purpose of this analysis is to identify regions of the fuel performance design space that have not yet been explored enough to make *generally-applicable* assertions about UCO-fueled TRISO performance under those conditions. Each application will differ, and it will ultimately fall on members of industry and regulators to demonstrate and confirm that its performance is acceptable. This analysis is intended to make that process more efficient by identifying and addressing potential issues in advance.

Gaps in our understanding of UCO-fueled TRISO performance during HTGR and non-HTGR transient operation are summarized below.

- It is not clear whether findings from historical transient tests performed with $UO_2$-fueled particles are directly applicable to modern UCO-fueled particles. $UO_2$ and UCO have different compositions, microstructures, and atomic bond strengths; and the particles have different structures, dimensions, and fabrication techniques—all of which could affect their transient performance. The in-pile performance of UCO-fueled particles at moderate and high heat rates (approximately 0.1-10 K/s and 10+ K/s, respectively) has not been observed directly.
- Historical test reactor irradiations convolute the effects of temperature and heat rate. The conditions were not representative of commercial power reactors, and it is difficult to determine accurate thermal histories for the samples, so their ability to bound fuel performance for commercial applications is limited.
- Data from historical tests performed in operating HTGRs are ideal for supporting ongoing HTGR

commercialization efforts. However, additional testing may be needed to characterize performance in regions of the parameter space applicable to different types of reactors or drastically-different HTGR designs and service conditions.

A multiphysics modeling and simulation workflow based on BISON and Griffin was developed to model TRISO fuel performance and aid in the design of targeted transient experiments capable of addressing these gaps. BISON was used to identify the power and temperature conditions needed to target specific regions of the transient parameter space by modeling TRISO fuel performance at both the compact and particle scales. A surrogate reactivity model based on Griffin was then used to determine the TREAT operating parameters (i.e., power, temperature, and control rod motion) needed to expose the fuel to the desired operating regime.

The workflow was first applied to simulate a reference transient for a prototypic HTGR to establish a baseline. It was then applied to identify and design a series of potential TREAT experiments that could be conducted to address the gaps noted above. These analyses are detailed in the following sections.

# 4. ANALYSIS OF THE REFERENCE TRANSIENT

The Griffin reactor multiphysics application was recently used to model power and fuel temperature evolution in response to a series of transients for a prototypic pebble bed-type HTGR [34]. Analyses included CRWs from cold-zero power (CZP) and hot-full power. The CRW from CZP transient was determined to be the most limiting from a fuel performance perspective due to the high heat rates and temperatures it produced in the fuel. Although this transient exceeds typical DBAs, which usually involve a partial withdrawal from the equilibrium position, it was the only scenario considered significant enough to warrant analysis using fuel performance tools. This scenario requires the reactor at equilibrium to shut down for several weeks to allow for Xe decay, reduce decay heat, and bring the fuel temperature down to the helium inlet temperature. It then requires a complete, simultaneous, and uninterrupted spurious withdrawal of all control rods at a rate of 1 cm/s, requiring several minutes without intervention to fully withdraw.

Notably, the analysis confirmed the stability and reliability of both the reactor and fuel designs. Nevertheless, the severity of the transient makes it ideal for exercising the multiphysics modeling workflow in the current work. The CRW from CZP transient, hereafter referred to as the *reference transient*, was reconstructed in BISON to model TRISO fuel performance at a fidelity exceeding that of the smeared compact-scale representation used to perform the original analyses. A workflow utilizing Griffin was then applied to determine the conditions necessary to conduct a representative transient experiment in TREAT. This analysis approach was adapted from a workflow recently developed to aid in the design of TREAT experiments for fuels used in nuclear thermal propulsion (NTP) systems [35, 36].

## 4.1. Fuel Performance Modeling

The BISON model geometry was adapted from the TREAT capsule design used in the earlier NTP work. The simplified geometry consists of three layers, including a titanium capsule, a zirconia liner, and a molybdenum flask. Simplified internals consisting of a tungsten sample holder and zirconia spacers were used to position a single AGR-2 compact within the capsule. The gaps between the solid bodies were assumed to be filled with Ar gas. This setup helps to insulate the TRISO compact from its surroundings, decreasing the power needed to achieve high heat rates and temperatures. The MOOSE `MultiApp` system was used to position a single TRISO particle at the center of the smeared compact (at the hottest location). The compact- and particle-scale geometries are shown in Figure 3.

Note that while the reference transient used pebble-type fuel, the current work focuses on cylindrical compacts like those used in the AGR program. Compacts like these have already been irradiated under prototypic conditions and may be available for follow-on transient testing. This change in compact form is not expected to have a significant impact on fuel performance at the particle scale. Using loose particles to

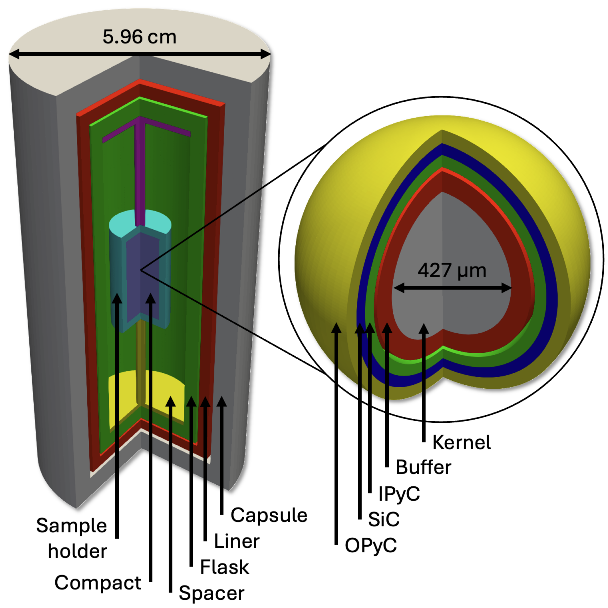


Figure 3. Schematic illustrating the two computational domains used for BISON analyses. A simplified TREAT capsule modified to accommodate a homogenized AGR-2 compact is shown on the left. The MOOSE `MultiApp` system was used to model a fully-resolved TRISO particle at the center of the compact, as shown on the right.

conduct transient experiments, as was done in historical test reactor irradiations, may be inadvisable because loose particles may fail at higher rates than those supported by matrix material. Transient experiments could potentially be conducted with smaller portions of compacts, but care would need to be taken to ensure that this type of testing is representative of full-compact behavior. While this approach would require less material per test, testing fewer particles would make it more difficult to collect meaningful failure statistics and validate quantitative failure probability predictions.

At the compact scale, BISON models transient conduction and radiation with heat generation. Material properties were taken from BISON whenever possible, and otherwise from the public references used by the earlier NTP work. The BISON classes applied at the compact scale are summarized in Table 1. These include thermal conductivity degradation in the TRISO compact due to irradiation. A full description of this and other models can be found in the extensive BISON documentation available online [37].

Table 1. Summary of physical behaviors and material properties included in the compact-level simulation and the BISON class(es) used to model each.

| Model | BISON class(es) |
|---|---|
| Conservation of energy | `HeatConductionTimeDerivative`, `HeatConduction`, and `HeatSource` |
| Meshed cavity radiation | `GrayDiffuseRadiation` |
| Unmeshed gap conduction and radiation | `GapHeatTransfer` |
| Density | `Density` |
| Thermal properties | `XThermal` and `HeatConductionMaterial` (`X` = `GraphiteMatrix`, `Molybdenum`) |

Reactor temperature, which is applied to the outside of the capsule, and power density, which is applied uniformly throughout the compact, supply the boundary conditions and forcing functions needed to drive the compact-scale simulation. The compact-scale simulation, in turn, drives the particle-scale simulation through the MOOSE `MultiApp` system. The spatially-resolved compact temperature is sampled at the particle location to provide a time-varying boundary condition, which is applied to the surface of the particle, linking the two scales.

At the particle scale, BISON models transient heat conduction with heat generation and finite deformation mechanics. The behaviors modeled include formation of a gap between the buffer and IPyC with appropriate thermal and mechanical contact constraints, irradiation effects such as fuel swelling, FGR and associated internal pressure buildup, and IPyC and OPyC irradiation-induced dimensional change (IIDC), which accounts for the irradiation-dependent Bacon anisotropy factor (BAF). UCO material properties and behavioral models were used whenever possible, and $UO_2$ models were used in cases where no UCO model was available or when the available UCO model did not fully support MOOSE `Restart` functionality. Use of selected $UO_2$ models is not expected to be a significant limitation at this stage of the work. Development of additional UCO-specific models is ongoing, and they will be incorporated into these analyses as they are made available. A full list of the BISON classes employed at the particle scale is given in Table 2. As before, full descriptions of these models, the theory behind them, and underlying references can be found in the online BISON documentation [37].

Table 2. Summary of physical behaviors and material properties included in the particle-level simulation and the BISON class(es) used to model each.

| Model | BISON class(es) |
|---|---|
| Conservation of energy | `HeatConductionTimeDerivative`, `HeatConduction`, and `NeutronHeatSource` |
| Conservation of momentum | `QuasiStaticAction` |
| Internal pressure | `PlenumPressureAction` |
| Buffer–IPyC mechanical contact | `ContactAction` |
| Buffer–IPyC gap conduction | `ThermalContactAction` |
| Density | `Density` |
| Thermal properties | `XThermal` and `HeatConductionMaterial` (`X` = `UCO`, `Buffer`, `MonolithicSiC`) |
| Thermal expansion | `UO2ThermalExpansionMATPROEigenstrain` and `XThermalExpansionEigenstrain` (`X` = `Buffer`, `PyC`, `MonolithicSiC`) |
| Elasticity | `XElasticityTensor` (`X` = `UCO`, `Buffer`, `PyC`, `MonolithicSiC`) |
| Creep | `XCreepUpdate` (`X` = `UO2`, `BufferCEGA`, `PyCCEGA`, `MonolithicSiC`) |
| Fuel burnup | `UCOBurnup` |
| Fuel FGR | `UO2Sifgrs` |
| Fuel swelling | `UCOVolumetricSwellingEigenstrain` |
| Buffer, IPyC, and OPyC IIDC | `XCEGAIrradiationEigenstrain` (`X` = `Buffer`, `PyCCEGA`) |
| IPyC and OPyC BAF | `BaconAnisotropyFactor` |

AGR-2 operating conditions obtained from the Nuclear Data Management and Analysis System (NDMAS) were used to simulate irradiation of the particle in the Advanced Test Reactor (ATR) using BISON [38]. Specifically, this work utilized time-resolved power density, temperature, and fast neutron fluence data from Compact 2-4-2, which achieved the highest burnup of the compacts irradiated during the AGR-2 experiment.

Simulating the ATR irradiation, hereafter referred to as the *steady-state* irradiation, allowed us to establish the initial conditions needed to model the transient response of irradiated TRISO fuel. These conditions could also be omitted to model the transient response of fresh TRISO fuel if desired.

Three common TRISO fuel performance metrics were selected for examination in this work: peak particle temperature, internal particle pressure, and tangential (hoop) stress in the IPyC, SiC, and OPyC. While BISON is capable of modeling additional behaviors associated with particle failure and predicting quantitative failure probabilities for populations of particles, the more general metrics listed above were deemed to be sufficient at this stage of the work. Evolution of the three metrics over the course of the steady-state irradiation, as predicted by BISON, is shown in Figure 4.

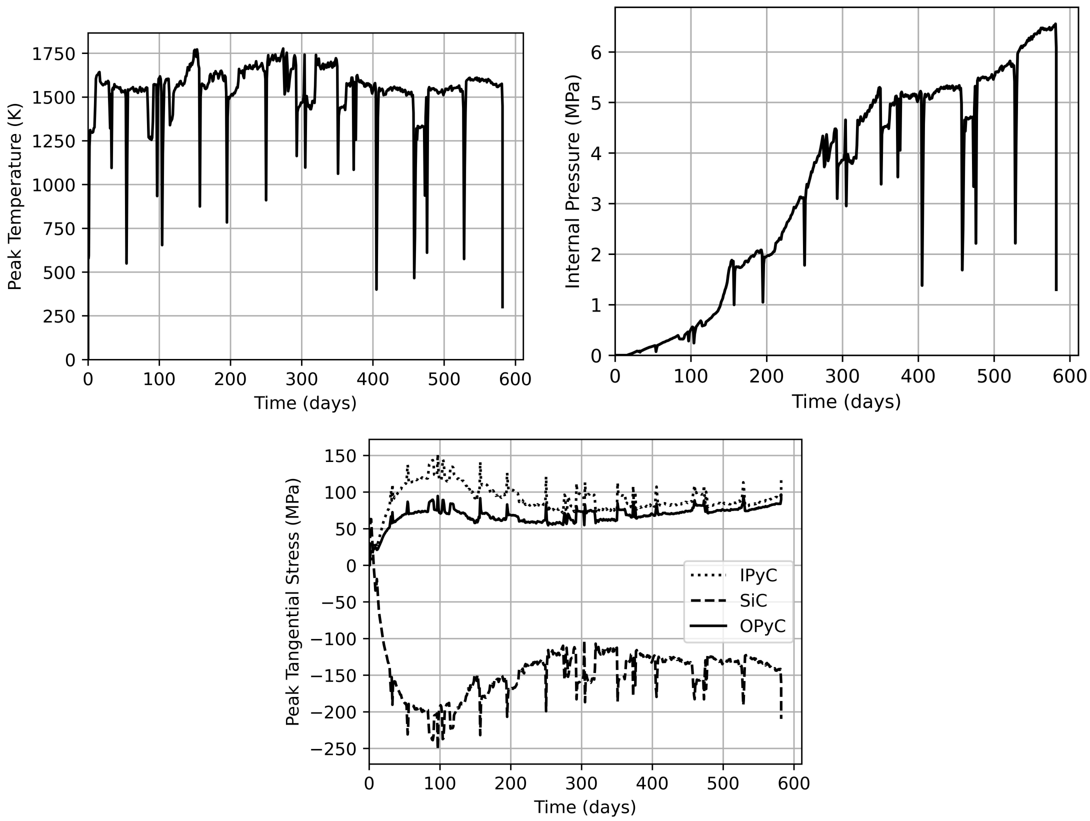


Figure 4. Evolution of three common fuel performance metrics during the steady-state AGR-2 irradiation: peak particle temperature, particle internal pressure, and peak tangential stress in the IPyC, SiC, and OPyC.

The vertical features in the temperature predictions reveal the high-fidelity time resolution of the operating conditions obtained from NDMAS. These features, which are associated with changes in ATR power and temperature, are also visible in the pressure and stress results. The particle generally sustained peak temperatures of about 1500-1700 K and achieved a peak internal pressure of about 6.5 MPa during the nearly 600-day steady-state irradiation. These temperatures are qualitatively consistent with compact-scale thermal analyses performed under the AGR program, which predicted that Compact 2-4-2 sustained one of the highest time-averaged, volume-averaged temperatures of all the AGR-2 compacts [38]. More rigorous comparisons between BISON and AGR thermal model predictions may be made in future work.

The stress predictions shown in Figure 4 are less intuitive. Early in the irradiation, the IPyC and OPyC begin to shrink in the tangential direction due to IIDC. This puts them in a tensile stress state and induces compressive stresses in the SiC to which they are bonded. Over time, creep tends to relax these stresses.

Meanwhile, pressure buildup in the buffer-IPyC gap due to FGR induces additional tensile stress in all three coating layers. The combined effects of these behaviors cause the tangential stress in the SiC to become less compressive over time. Nevertheless, the SiC stress remains well within the compressive regime. This is desirable because compressive stress states preclude the formation of cracks associated with particle failure. Overall, the steady-state results presented here are consistent with those obtained using BISON previously [7] and the general understanding of UCO-fueled TRISO performance [39].

With the problem domains and initial conditions in place, BISON was used to reconstruct the conditions of the reference transient within the TREAT capsule setup. Computational-analogs for two existing TREAT capabilities were leveraged to establish the necessary conditions: resistive sample heating and power shaping [40, 41]. Resistive sample heating can be applied to elevate capsule temperature up to about 1000 K. Preheating from room temperature at the end of the steady-state irradiation to the reference transient initiation temperature of 550 K was performed at a rate of 0.01 K/s to demonstrate how temperature conditions can be established while minimizing the effects of any material behaviors that may be sensitive to higher heat rates. Similarly, a piecewise power density history requiring TREAT power-shaping capabilities was constructed to reproduce the desired transient thermal behaviors. The resulting temperature and heat rate predictions are compared to compact-scale values extracted from the reference transient in Figure 5.

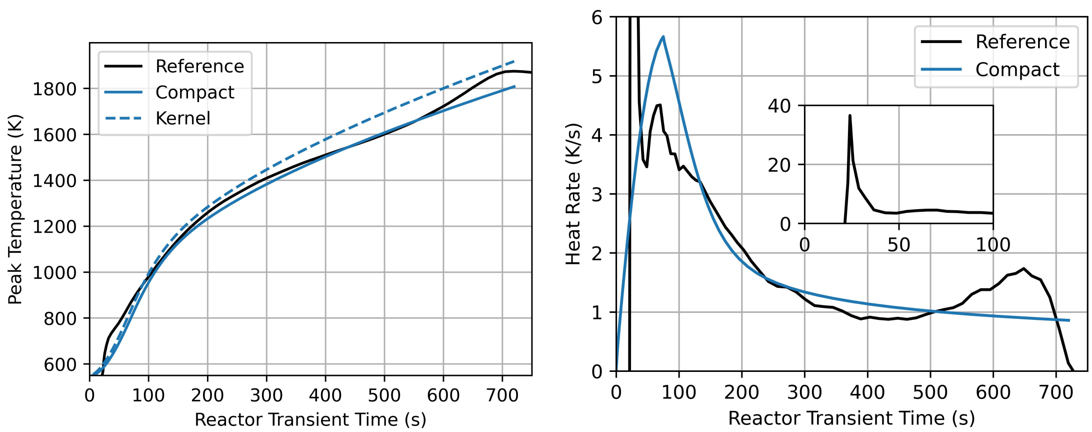


Figure 5. Comparisons between the peak temperatures and heat rates predicted for the reference transient in the current work and values extracted from the reference [34]. The comparisons show that the BISON simulation adequately represents the reference transient, except for omission of a momentarily-high heat rate at about 30 s, which is shown in the inset. Here, *reactor transient time* denotes the duration of simulated reactor operation, which excludes the time spent preheating the sample from room temperature to the transient initiation temperature given in the reference.

The temperature results show that the simulation reproduces peak compact temperature evolution with a reasonable degree of accuracy. The horizontal axis in each plot, *reactor transient time*, denotes the duration of simulated reactor operation, which excludes the time spent preheating the sample. The results also show the peak kernel temperature, which is elevated above and tracks well with the compact temperature. The BISON-predicted heat rate likewise agrees reasonably well with that of the reference, except for omission of a momentarily-high heat rate at about 30 s. More precise control of transient conditions could be obtained by refining the reactor temperature and power density functions. However, this level of consistency is considered satisfactory at this time, as the current work focuses more on demonstrating the capabilities needed to design targeted transient experiments than on a detailed analysis of this particular transient.

Figure 6 shows how the fuel performance metrics evolve during the transient. Steady-state fuel performance predictions are also included for comparison. Each horizontal axis is split into two parts: the

steady-state irradiation time in days and the *transient time* in hours, which includes the time spent in both the preheating and irradiation stages of the simulated transient experiment.

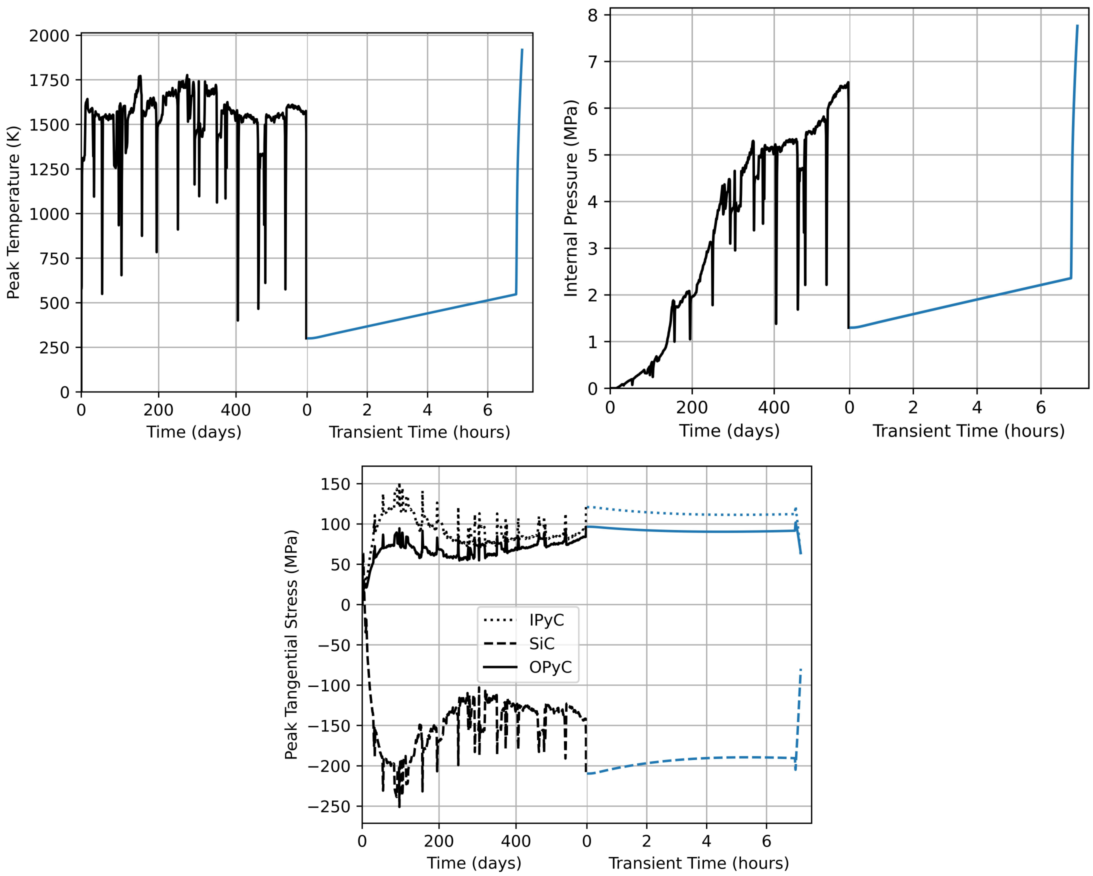


Figure 6. Evolution of three common fuel performance metrics during the steady-state AGR-2 irradiation and the subsequent reference transient. Here, *transient time* denotes the total time spent preheating and irradiating the sample in TREAT. The results show that BISON predicts a higher temperature, higher internal pressure, and less-compressive tangential stress in the SiC during the transient than during the steady-state irradiation.

The temperature results show that the time required to preheat the sample (approximately 6.5 hours) is much longer than the time needed to irradiate it (approximately 12 minutes, as shown in Figure 5). The preheat time could be reduced significantly by utilizing a heat rate higher than 0.01 K/s once it is confirmed that doing so does not impair efforts to deconvolute transient temperature and heat rate effects. Thermal data collected during AGR experiments involving ATR startup and post-irradiation high-temperature testing may be leveraged to help relax this constraint in future work.

Increasing the preheating rate would have the added benefit of reducing the overall time needed to conduct these experiments in TREAT. Overall, the results show that for this specific case, the transient irradiation produces more limiting fuel performance behaviors than were observed during the steady-state irradiation. Specifically, the transient produced a higher peak temperature, higher internal pressure, and less-compressive tangential stress in the SiC. Nevertheless, each parameter remained within acceptable limits.

When considering the results shown in Figure 5 and Figure 6 together, the limiting fuel performance behaviors appear to correlate more to the highest temperature, which is present toward the end of the transient irradiation, than to the highest heat rate, which is present toward the beginning. As run, the particle-scale BISON model captures only a subset of the behaviors that could reasonably be sensitive to high heat rates.

Specifically, it accounts for differential thermal expansion of TRISO layers but does not include models for the weaker bonds that may exist between TRISO layers, fuel micro-cracking, or transient FGR. These behaviors will be explored further in future work.

Transient experiments would be needed to confirm the accuracy of these predictive capabilities and improve them as necessary. The analyses presented in this section demonstrate how BISON models can be applied to identify the experimental conditions (i.e., reactor temperature and power density) needed to target fuel performance behaviors of interest. In the next section, we demonstrate how surrogate reactivity modeling can be applied to determine the TREAT power and control rod motion necessary to conduct these types of experiments.

## 4.2. TREAT Predictive Transient Modeling

In this work, we utilized a methodology developed for the analysis of a series of NASA-sponsored Sirius NTP fuel experiments conducted at TREAT [35, 36]. The predictive transient model of TREAT incorporates multiple constituent models, including high fidelity and reduced-order models, to provide accurate predictions of reactor power, temperature, deposited energy, axial control rod movement, and specimen temperature. The model was initially introduced and validated for NTP fuel applications in previous studies of Sirius-1, 2c, and 3 [35, 36]. The model includes three primary components: (1) surrogate models and data generation, (2) TREAT predictive transient model, and (3) specimen temperature predictive model. Figure 7 shows a schematic diagram illustrating the calculation workflow of the model, and Table 3 provides a description of each component of the model.

TREAT features a central irradiation position that allows for experimental irradiation and material testing with high neutron flux levels [42]. It supports two primary categories of transients: exponential bursts and shaped power bursts. Exponential bursts are temperature-limited excursions, where the control rods are dropped to terminate the transient before the temperature limit is reached, or to limit the energy deposited at the end of the transient. Shaped power bursts are generated by an initial step insertion of reactivity, followed by reactivity adjustments to achieve the desired burst shape. A flattop transient is a type of shaped transient, characterized by maintaining a constant elevated core power for a duration longer than that of an exponential burst transient. TREAT transients can be customized to vary in both power and duration, constrained only by their core energy capacity or the maximum permissible enthalpy rise of up to 2.5 GJ. This capability allows for simulating accident conditions in test specimens without exceeding fuel and cladding temperature limits [43, 44].

The primary purpose of the predictive transient model of TREAT is to determine the axial movement of the control rods to achieve desired transient conditions without violating TREAT operational limits. To calculate the temperature evolution within the specimen being irradiated in TREAT, the power deposited within the specimen must be provided. The specimen power is calculated from the reactor power using a power coupling factor, i.e., the ratio of the fission reaction rate in the specimen to that in the reactor. The power coupling factor is calculated from high fidelity models of TREAT [45] and the specimen using Serpent Monte Carlo code [46]. Figure 8 shows radial and axial views of the TREAT Serpent model with the experiment positioned at the central irradiation location.

The TREAT predictive transient model was applied to the reference transient using the power density history determined by BISON to calculate a power coupling factor of 22.4 W/MW. The analysis determined that the transient would violate the enthalpy rise limit of TREAT. The low power coupling factor is believed to result from the low average fissile atom density in the TRISO compact compared to samples examined in the previous NTP work. This highlights a challenge associated with TRISO transient testing in TREAT and the importance of the BISON–Griffin workflow demonstrated herein. In the next section, we leverage this power coupling information to demonstrate how the workflow can be applied to identify transients that could potentially be performed in TREAT without violating its operational limits.

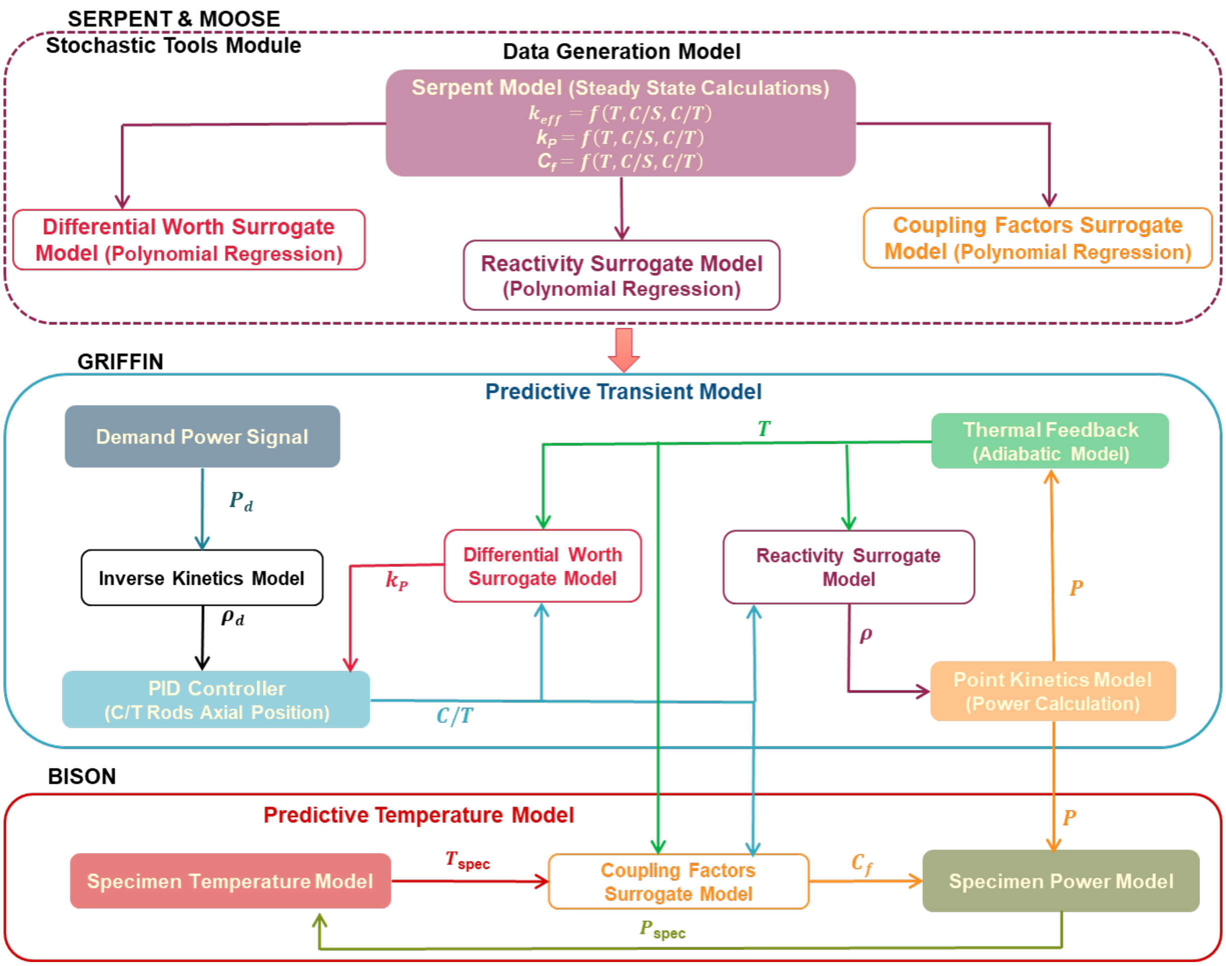


Figure 7. Illustration of the TREAT predictive transient model calculation workflow [35, 36].

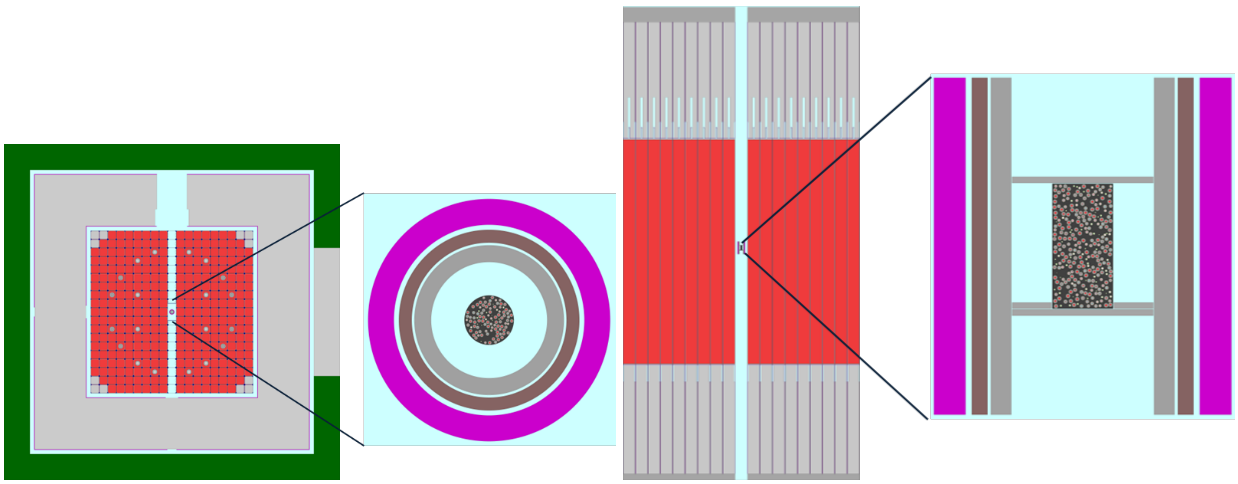

(a) Radial view (XY) (b) Axial view (XZ)

Figure 8. Radial and axial views of the Serpent model used to analyze the TRISO compact in TREAT.

Table 3. Description of the TREAT predictive transient model components and submodels.

| Component/Model | Description |
|---|---|
| TREAT Serpent model | Provides the necessary datasets to train the developed surrogate models based on positions of control rods, average reactor temperature, and average specimen temperature |
| Differential surrogate model | Performs polynomial regression on tabulated data to compute differential rod worth coefficients |
| Reactivity surrogate model | Performs polynomial regression on precalculated steady-state eigenvalue data sets to predict the reactivity introduced into the system |
| Coupling factors surrogate model | Performs polynomial regression on power coupling factors for experiment computed by Serpent |
| Inverse kinetics model | Converts the demand power signal into a reactivity demand signal using given kinetics parameters and the time step size |
| Proportional controller | Determines the equivalent reactivity of control rod axial movement in response to the calculated demand reactivity signal |
| Adiabatic thermal feedback model | Computes the average reactor temperature given the heat deposited in the system at each time point |
| Point kinetics model | Computes the total power and concentrations of delayed neutron precursors based on the predicted reactivity introduced into the system at each time point |
| Specimen power model | Calculates the specimen power based on the predicted coupling factor and the total reactor power |
| Specimen thermal model | Calculates the specimen temperature using the specimen power and a detailed thermal model of the specimen |

In the current work, BISON was used to determine the required specimen power to achieve a desired temperature and heating rate. The desired power signal of the reactor was then determined using the power coupling factors calculated with the high fidelity Serpent model. Finally, the TREAT predictive transient model was used to determine the axial control rod movement needed to achieve the desired power signal without violating the core energy capacity limit. This workflow helps in designing the experiment and ensuring it lies within the operational limits of TREAT, which requires some iteration between the models. The BISON model and the TREAT predictive transient model are not yet coupled directly. The specimen power is directly coupled to the reactor power, while the reactor temperature change is not yet considered in the BISON model of the specimen. This is acceptable at this stage of the work because accounting for reactor heat up only lessens the reactor power required to achieve target heat rates. However, this will be taken into consideration when refining the BISON–Griffin workflow in future work.

# 5. ANALYSIS OF POTENTIAL TREAT TRANSIENTS

Given the current experimental setup, the analyses presented in the previous section indicate that the power and time required to reproduce the reference transient cannot be supplied by TREAT without exceeding the core energy deposition limit. Nevertheless, existing TREAT capabilities should be adequate to conduct different transient experiments that reproduce key features of the reference transient. This represents an opportunity to address some of the gaps identified above by designing more generally-applicable transient

experiments. Ideally, these experiments would collect data that relate key fuel performance behaviors directly to observable operational parameters like transient initiation temperature and heat rate, reducing the need to consider each combination of reactor type and transient type separately.

This approach would:

- Collect the data needed to confirm or refine our understanding of UCO-fueled TRISO performance, and therefore, validate or incorporate additional transient-specific models into our predictive capabilities
- Establish a baseline database for UCO-fueled TRISO performance
- Provide a valuable fuel performance database that stakeholders could use to support the design of their fuels and reactors.

To that end, the reference transient was examined in greater detail and within the context of the gaps identified above to develop a matrix of potential TRISO transient experiments that could be conducted in TREAT. The BISON–Griffin workflow developed in the previous section was then applied to determine how TREAT could be operated to conduct these experiments, and to demonstrate how the resulting experimental data could be leveraged to validate and/or further develop the fuel performance models.

## 5.1. Fuel Performance Modeling

The peak heat rate achieved in the BISON simulation of the reference transient in the previous section was approximately 5 K/s. Further analysis of the thermal history from the reference transient revealed a momentarily-high heat rate of approximately 35 K/s early in the simulated CRW. As previously noted, resistive heating can be applied to elevate capsule temperature up to about 1000 K. These and intermediate values were developed into a matrix of possible TRISO transient experiments, which is shown in Table 4.

Table 4. Example experiment matrix based on characteristic values from the reference transient. TREAT resistive-preheating and power-shaping capabilities can be leveraged to precisely control transient initiation temperature and heat rate, enabling studies that could deconvolute the roles of the two parameters and facilitate model development and validation.

| Transient Initiation Temperature (K) | Peak Heat Rate (K/s) 5 | 20 | 35 |
|---|---|---|---|
| 300 | | | |
| 650 | | | |
| 1000 | | | |

The experiment matrix addresses many of the transient performance gaps identified in Section 3. Specifically, these experiments would provide direct evidence of UCO-fueled particle performance at moderate to high heat rates and should allow for the roles of temperature and heat rate to be deconvoluted. Similar tests could be performed with $UO_2$-fueled particles from AGR-2 to help determine whether historical $UO_2$ transient testing can be leveraged to support qualification of UCO-fueled particles.

Post-irradiation examination data from these experiments (both quantitative failure probability analyses and qualitative evidence of failure mechanisms) could then be leveraged to support code validation and refine TRISO fuel performance models as needed. It should be noted that validating quantitative failure probability predictions requires a statistically-significant number of failure observations, which could be obtained from either a smaller number of tests with more extreme conditions or a larger number of tests with milder conditions. Care should taken to balance (1) the need for validating quantitative failure probability predictions, (2) the need to conduct testing under realistic transient conditions, and (3) the overhead associated with the proposed testing when eventually designing a transient test plan. The codes could then be leveraged

to interpolate within the TRISO transient design space to assess the performance of specific fuel designs under specific conditions.

The multiscale BISON model and power coupling factor introduced in the previous section were then applied to iteratively determine the power densities necessary to deliver the desired experimental conditions. As before, samples were preheated to transient initiation temperature at a rate of 0.01 K/s. Power was then rapidly increased over a period of 5 s and held constant until initiating a 5 s shutdown. This particular setup was selected for demonstration purposes and can be adjusted as needed to accommodate additional TREAT requirements. Peak powers were chosen using the BISON-predicted heat rates, and the total length of each transient was determined by the TREAT energy deposition limit. Evolution of the selected fuel performance metrics during the transients is shown in Figure 9. Therein, the nine cases are labeled according to their transient initiation temperature $T_0$ and peak heat rate $(\Delta T/\Delta t)$.

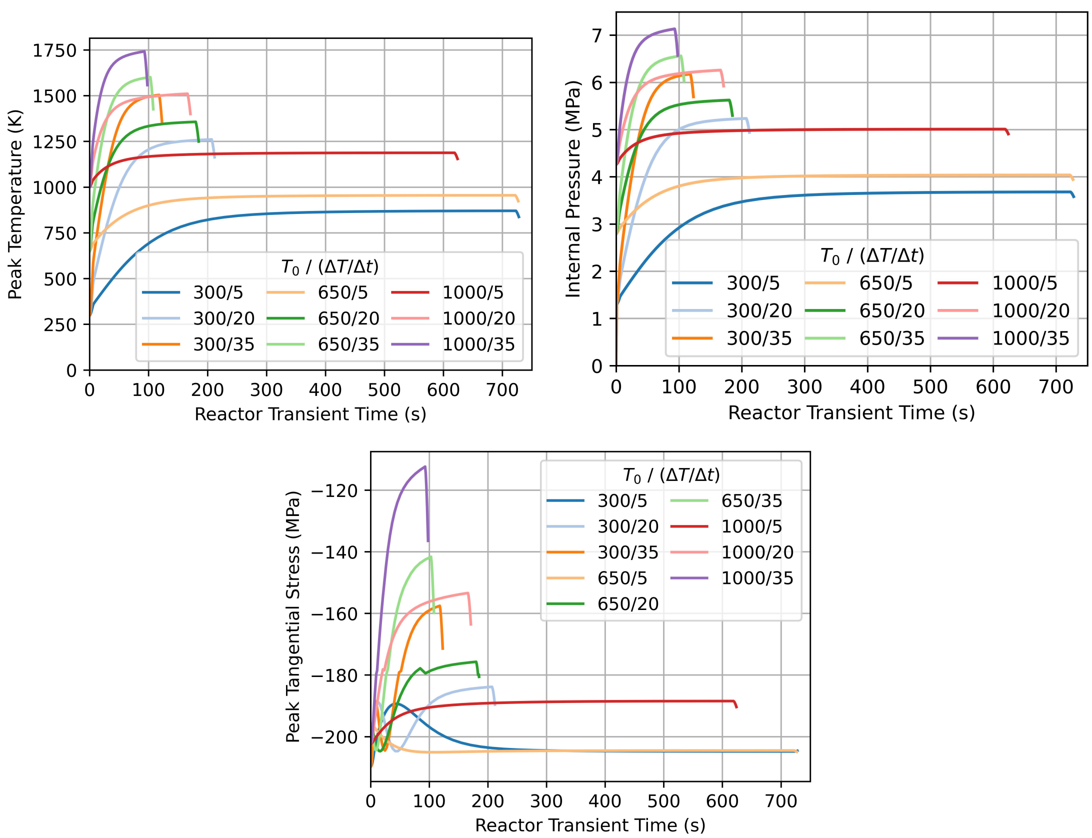


Figure 9. Evolution of three common fuel performance metrics predicted for the experiments outlined in Table 4. Here, $T_0$ denotes the transient initiation temperature, and $(\Delta T/\Delta t)$ denotes the peak heat rate. The stress predictions are for the SiC layer.

The results include only the powered portions of the tests. The temperature results show that heat rates were highest early in the tests and temperature tended to level off during the flat-top transient. Tests with the most preheating and highest heat rates produced the highest peak temperatures, as expected. The tests with lower heat rates were permitted to run for longer because they required less power, but they could be shortened for consistency with the other tests if desired. The lengths of the shutdowns could also be modified to control sample temperature during cool-down.

As was the case with the reference transient, the trends in the pressure results follow those of the temperature results very closely. The stress predictions show that the transients are expected to produce

less-compressive stresses in the SiC layer. The magnitudes and evolution of the stress effects depend strongly on temperature and heat rate in complex ways due to the combined effects of internal pressure buildup, differential thermal expansion, and elastic and inelastic deformation. Figure 10 shows the instantaneous thermal expansion coefficients of pyrolytic carbon (PyC) (in the tangential direction) and SiC over the range of temperatures encountered in the transients. The figure also shows another view of the predicted tangential stresses in the SiC, which includes both the time spent preheating the sample and a portion of the time immediately following reactor startup. Each data set is discussed in further detail below to help interpret the transient stress predictions shown in Figure 9.

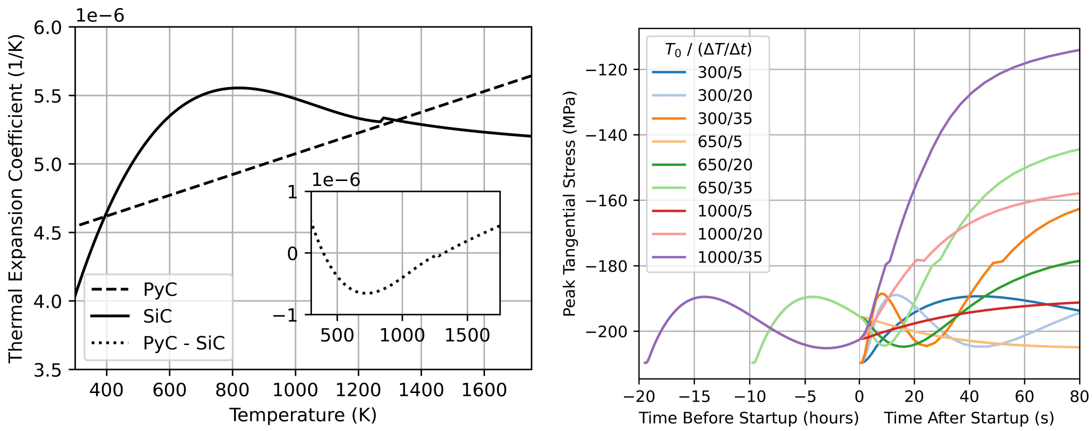


Figure 10. The instantaneous thermal expansion coefficients of PyC (in the tangential direction) and SiC as predicted by BISON and another view of SiC tangential stress evolution during sample preheating and immediately following reactor startup. The inset in the thermal expansion plot shows the thermal expansion mismatch, which is given by the PyC coefficient minus the SiC coefficient.

The tangential component of the anisotropic PyC thermal expansion coefficient at this fast neutron fluence and BAF is essentially linear over the temperature range and increases with temperature. The isotropic SiC coefficient exhibits significant nonlinearities and has a small discontinuity at about 1300 K due to the piecewise correlation used to model it. The mismatch between them, which is given by the PyC coefficient minus the SiC coefficient, is initially positive and then crosses zero at about 400 K and 1300 K. As such, heating an initially stress-free sample of bonded PyC and SiC from room temperature would be expected to put the SiC in tension at low temperatures, followed by compression at intermediate temperatures, and finally tension at high temperatures.

The second view of the tangential stresses in the SiC accounts for the transients' varying preheat times by aligning all reactor startups at zero. The difference in time scales before and after reactor startup highlights the slow preheat rate selected for these demonstrations. As expected, the thermal and stress histories associated with transients initiated at each temperature overlap prior to reactor startup and diverge quickly thereafter. For each transient, the stress in the SiC is initially compressive due to the substantial inelastic strains accumulated in the PyC layers during the steady-state irradiation. The three-regime thermal expansion mismatch discussed above contributes to less-compressive, then more-compressive, and finally less-compressive stress in the SiC as the samples increase in temperature. Major differences in sample behavior after reactor startup can be attributed to the combined effects of thermal expansion mismatch and internal pressure as functions of temperature and heat rate.

These observations help to explain the stress behaviors of the $T_0/(\Delta T/\Delta t)$ = 300/5 and 650/5 transients, which are unusual when compared to the others. Examination of the temperature, thermal expansion, and stress data in Figure 9 and Figure 10 shows that these two samples did not accumulate sufficient thermal

energy to enter into the third thermal expansion mismatch regime, and the the stresses in the SiC layers therefore remain highly compressive. The complexity of these behaviors highlights the usefulness of applying detailed fuel performance models like BISON to aid in designing transient experiments and interpreting data from them.

It should be noted that, for convenience, all simulation results presented in this work were obtained using stress free temperatures equal to the reference transient initiation temperature (approximately 550 K). In reality, the stress free temperatures used to predict thermal expansion are functions of fabrication variables like layer deposition temperature and may be affected by annealing during fabrication or irradiation. These factors impact residual stress in unirradiated TRISO particles and stress evolution thereafter. While a thorough analysis of these properties and behaviors is beyond the scope of this work, the authors recommend investigating them in more detail in the future.

## 5.2. TREAT Predictive Transient Modeling

The predictive transient model of TREAT was employed to determine the desired transient operating conditions, while observing the core energy deposition limit of 2.5 GJ. Initially, the multiscale BISON model was utilized to determine the desired power density within the specimen. This power density was then converted into a desired reactor power signal using pre-calculated coupling factors. With this desired reactor power signal, the predictive transient model was applied to determine the movement of the control rods to reproduce the power signal and to ensure that the deposited energy remained within operational limits.

A flattop transient of TREAT was selected to determine the necessary power level and movement of the control rods. Figure 11 illustrates the reactor power, total deposited energy, average core temperature, and predicted control rod position and speed for each of the nine potential transients. For each transient case, the power was ramped up exponentially over 5 seconds and then held constant until the TREAT energy deposition limit was reached. Subsequently, the control rods were inserted to shut down the reactor and reduce power. Initially, the control rods were withdrawn to introduce sufficient positive reactivity to increase the reactor power to the desired level. This was followed by reinsertion of the control rods to maintain a constant power level. As the reactor heated up and the reactor fuel temperature increased, the control rods were withdrawn further to balance the negative reactivity feedback of the heated fuel, maintaining the same power level for the duration of the transient.

In all test cases, the power level remained constant while the control rod position stayed within the operational range (within 40 inches). The current model limits the movement range of the control rods axially, but does not limit the speed of the control rods. This might cause the large step move of the control rods at the beginning of the transient in certain situations, such as when the reactor power is ramped up in very short period of time, which will introduce a nonphysical control rod movement. In the current analysis, the reactor power is ramped exponentially to the desired level without exceeding the maximum speed of the control rods for all the transient cases, as shown in Figure 11. For all the potential transient cases, the maximum control rod speed is less than 1.6 m/s. In future updates of the TREAT predictive transient model, additional models will be included to ensure that the speed of the control rods does not violate the operational limits of TREAT for any suggested transient case, including the total energy deposition limit.

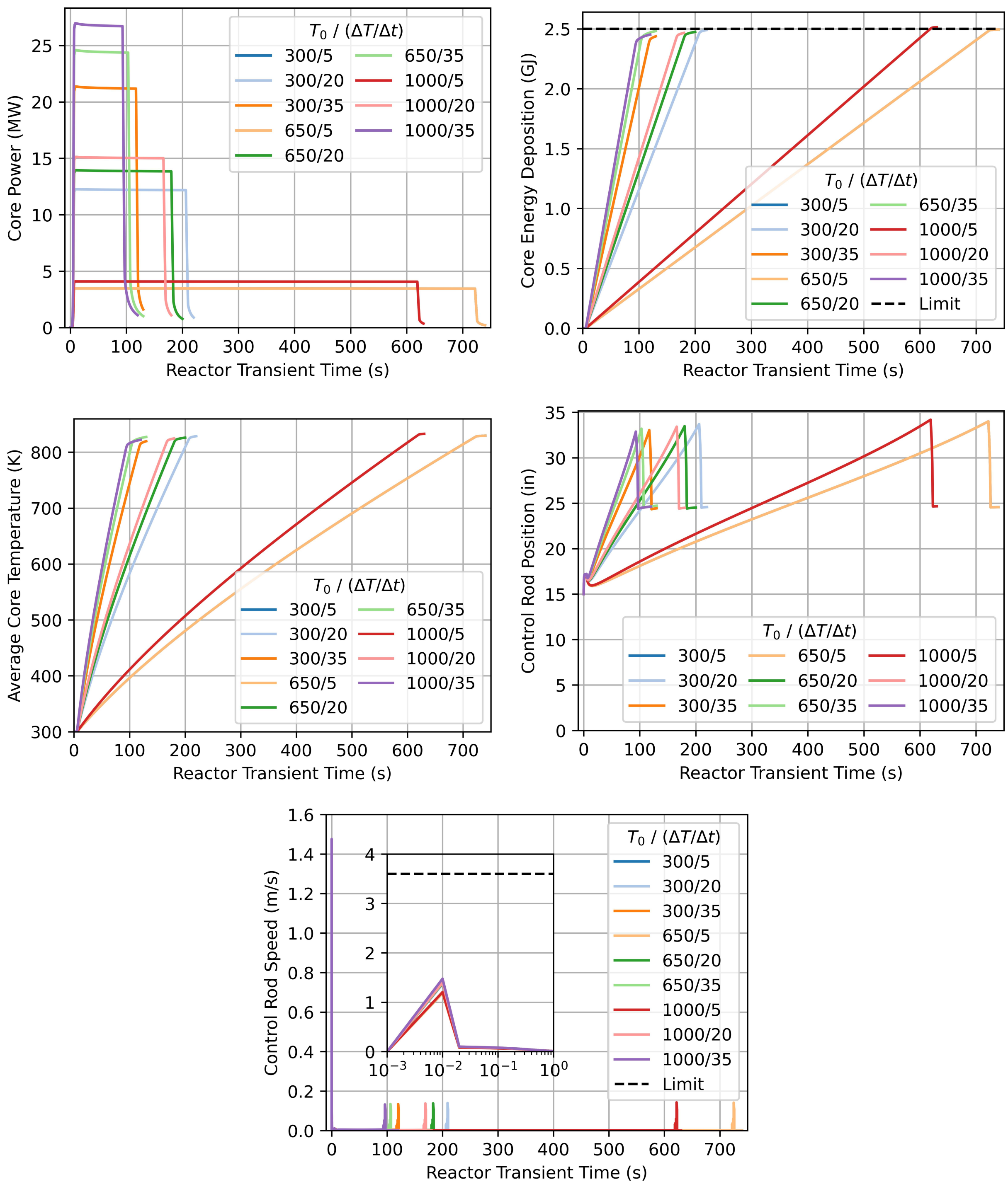


Figure 11. Evaluation of reactor operation conditions, including reactor power, total deposited energy, average core temperature, and control rod movement and speed for the experiments outlined in Table 4.

# 6. CONCLUSIONS AND FUTURE WORK

UCO-bearing TRISO particle fuels are expected to be used in numerous U.S. commercial reactor applications within the next decade. This work reviewed historical particle fuel transient experiments

to identify gaps in the TRISO transient fuel performance design space with the potential to hinder near-term deployment. Notable gaps include (1) questions about whether historical tests conducted with $UO_2$-fueled particles are relevant for modern UCO-fueled particles, (2) lack of experimental data for UCO-fueled particles at moderate and high heat rates, and (3) uncertainties regarding the thermal histories of early test reactor irradiations, which make it difficult to interpret their results and apply them to support qualification of fuels for commercial power reactors.

A BISON–Griffin modeling framework was developed to conduct preliminary TRISO transient analyses and begin to address the gaps described above. The framework was demonstrated using limiting-case transient conditions for a prototypic HTGR. Predicted particle temperatures, internal particle pressures, and tangential stresses in the structural layers were examined for a particle initialized with conditions from the steady-state AGR-2 irradiation. The limiting fuel performance behaviors appeared to correlate more to high temperature than to high heat rate. It should be noted that heat rate-sensitive behaviors such as fuel micro-cracking and transient FGR, which have been observed in other ceramic fuels, have not yet been applied to TRISO fuels and were therefore not included in these analyses.

The modeling framework was then applied to calculate the TREAT–sample power coupling factor and determine how TREAT would need to be operated to reproduce the conditions expected in the reference transient. The analysis showed that the low fissile density of the TRISO fuel produces weak power coupling with the TREAT core. As a result, the transient cannot be performed in TREAT using the current experiment design without violating the core energy deposition limit. As such, the modeling framework was then applied to develop a matrix of experiments that could potentially be performed in TREAT to (1) evaluate UCO-fueled particle performance at moderate and high heat rates, (2) assess whether historical testing with $UO_2$ is applicable to UCO, (3) deconvolute the roles of transient temperature and heat rate, and (4) collect the data needed for fuel performance model validation and/or further development.

Future work in this area falls into two categories: fundamental and practical. The current work focuses on how the operating conditions (i.e., temperature and heat rate) to which TRISO particles are exposed may impact their transient performance. It is highly likely that the materials, geometry, and irradiation history of particles also influence their transient performance. Examples may include burnup and thermal/irradiation history, which may impact transient initial conditions through their influence on thermomechanical properties and accumulation of fission product-induced degradation, such as Pd penetration. The authors recommend assessing additional parameters to construct a comprehensive TRISO transient design space, within which historical experiments, proposed engineering applications, and new tests can be situated.

The authors also recommend practical enhancements and refinements to the multiphysics modeling workflow demonstrated herein. These may include refining the predictive TREAT model to observe control rod speed limits, coupling reactor temperature feedback predicted by the surrogate reactivity model back into BISON, and iterating with TREAT staff to refine the capsule and sample designs. Instrumented experiments could also be conducted to confirm that the desired temperatures and heat rates can be reliably achieved prior to applying these methods to assess transient TRISO performance. These tasks are intended to maximize the readiness of TRISO transient analysis tools and experimental capabilities such that any testing, model development, or model validation deemed necessary can be conducted as efficiently as possible.

# 7. REFERENCES


[1] T. Pham, C. B., Palmer, J., Marshall, D. W., Hawkes, G. L., Scates, D. M., and Demkowicz, P. A., AGR-5/6/7 Irradiation Test Final As-run Report. Technical Report INL/EXT-21-64221, Idaho National Laboratory (2021).

[2] Demkowicz, P. A., Liu, B., and Hunn, J. D. (2019) Coated particle fuel: Historical perspectives and current progress. *Journal of Nuclear Materials,* **515**, 434–450.

[3] Powers, J. J. and Wirth, B. D. (2010) A review of TRISO fuel performance models. *Journal of Nuclear Materials,* **405**(1), 74–82.

[4] Williamson, R. L., Hales, J. D., Novascone, S. R., Pastore, G., Gamble, K. A., Spencer, B. W., Jiang, W., Pitts, S. A., Casagranda, A., Schwen, D., Zabriskie, A. X., Toptan, A., Gardner, R., Matthews, C., Liu, W., and Chen, H. (2021) BISON: A Flexible Code for Advanced Simulation of the Performance of Multiple Nuclear Fuel Forms. *Nuclear Technology,* **207**(7), 954–980.

[5] Permann, C. J., Gaston, D. R., Andrš, D., Carlsen, R. W., Kong, F., Lindsay, A. D., Miller, J. M., Peterson, J. W., Slaughter, A. E., Stogner, R. H., and Martineau, R. C. (2020) MOOSE: enabling massively parallel multiphysics simulation. *SoftwareX,* **11**, 100430.

[6] Hales, J., Williamson, R., Novascone, S., Perez, D., Spencer, B., and Pastore, G. (2013) Multidimensional multiphysics simulation of TRISO particle fuel. *Journal of Nuclear Materials,* **443**(1), 531–543.

[7] Jiang, W., Hales, J. D., Spencer, B. W., Collin, B. P., Slaughter, A. E., Novascone, S. R., Toptan, A., Gamble, K. A., and Gardner, R. (2021) TRISO particle fuel performance and failure analysis with BISON. *Journal of Nuclear Materials,* **548**, 152795.

[8] Lee, C., Jung, Y. S., Park, H., Shemon, E. R., Ortensi, J., Wang, Y., Laboure, V. M., and Prince, Z. M., Griffin Software Development Plan. Technical Report INL/EXT-21-63185, Idaho National Laboratory (2021).

[9] Wang, Y., Schunert, S., Ortensi, J., Laboure, V., DeHart, M., Prince, Z., Kong, F., Harter, J., Balestra, P., and Gleicher, F. (2021) Rattlesnake: A MOOSE-based multiphysics multischeme radiation transport application. *Nuclear Technology,* **207**(7), 1047–1072.

[10] Brown, N. R. (2020) A review of in-pile fuel safety tests of TRISO fuel forms and future testing opportunities in non-HTGR applications. *Journal of Nuclear Materials,* **534**, 152139.

[11] Smith, C. L., Fuel particle behavior under normal and transient conditions. Technical Report GA-A12971, General Atomics (1974).

[12] Fukuda, K., Hayashi, K., and Shiba, K. (1990) Fuel behavior and fission product release under HTGR accident conditions, Hemisphere Publishing, 79 Madison Avenue, New York, NY 10016 (USA).

[13] Umeda, M., Sugiyama, T., Nagase, F., Fuketa, T., Ueta, S., and Sawa, K. (2010) Behavior of Coated Fuel Particle of High-Temperature Gas-Cooled Reactor under Reactivity-Initiated Accident Conditions. *Journal of Nuclear Science and Technology,* **47**(11), 991–997.

[14] Agency, I. A. E. (1997) Fuel Performance and Fission Product Behaviour in Gas-Cooled Reactors, Number 978 in TECDOC Series—International Atomic Energy Agency, Vienna.

[15] Krüger, K., Bergerfurth, A., Burger, S., Pohl, P., Wimmers, M., and Cleveland, J. C. (1991) Preparation, Conduct, and Experimental Results of the AVR Loss-of-Coolant Accident Simulation Test. *Nuclear Science and Engineering,* **107**(2), 99–113.

[16] Hu, S., Wang, R., and Gao, Z. (2006) Transient tests on blower trip and rod removal at the HTR-10. *Nuclear Engineering and Design,* **236**(5), 677–680 HTR-2004.

[17] Gou, F., Liu, Y., Chen, F., and Dong, Y. (2018) Thermal behavior of the HTR-10 under combined PLOFC and ATWS condition initiated by unscrammed control rod withdrawal. *Nuclear Science and Techniques,* **29**(9).

[18] Fukuda, K., Kashimura, S., Tobita, T., and Kikuchi, T. (1995) Irradiation behavior of HTGR coated particle fuel at abnormally high temperature. *Nuclear Engineering and Design,* **157**(1), 221–230.

[19] Nakagawa, S., Takamatsu, K., Tachibana, Y., Sakaba, N., and Iyoku, T. (2004) Safety demonstration tests using high temperature engineering test reactor. *Nuclear Engineering and Design,* **233**(1), 301–308 Japan's HTTR.

[20] Schappel, D., Brown, N., and Terrani, K. (2020) Modeling reactivity insertion experiments of TRISO particles in NSRR using BISON. *Journal of Nuclear Materials,* **530**, 151965.

[21] Ghezzi, C. G., Schappel, D., Pastore, G., Wirth, B. D., and Brown, N. R. (2022) Sensitivity analysis applied to SiC failure probability in TRISO modeled with BISON. *Progress in Nuclear Energy,* **153**, 104431.

[22] Gorton, J. P. and Brown, N. R. (2020) Defining the performance envelope of reactivity-initiated accidents in a high-temperature gas-cooled reactor. *Nuclear Engineering and Design,* **370**, 110865.

[23] Carlotta G. Ghezzi, R. F. K. and Brown, N. R. (2022) TRISO SiC Failure Probability for Reactivity Initiated Accidents in High-Temperature Gas-Cooled Reactors. *Nuclear Science and Engineering,* **196**(11), 1361–1382.

[24] Carlotta G. Ghezzi, B. D. W. and Brown, N. R. (2024) TRISO Burnup-Dependent Failure Analysis of a HTGR Design-Basis Accident Using BISON. *Nuclear Science and Engineering,* **198**(5), 1036–1050.

[25] Brown, N. R., Betzler, B. R., Carbajo, J. J., Wysocki, A. J., Greenwood, M. S., Gentry, C., and Qualls, A. L. (2017) Preconceptual design of a fluoride high temperature salt-cooled engineering demonstration reactor: Core design and safety analysis. *Annals of Nuclear Energy,* **103**, 49–59.

[26] Ghezzi, C. G. and Brown, N. R. (2023) TRISO burnup-dependent failure analysis in FHRs using BISON. *Journal of Nuclear Materials,* **586**, 154651.

[27] Besmann, T., Ferber, M., Lin, H., and Collin, B. (2014) Fission product release and survivability of UN-kernel LWR TRISO fuel. *Journal of Nuclear Materials,* **448**(1), 412–419.

[28] Collin, B. P., AGR-1 Irradiation Test Final As-Run Report. Technical Report INL/EXT-10-18097, Rev. 3, Idaho National Laboratory (2015).

[29] Collin, B. P., AGR-2 Irradiation Test Final As-Run Report. Technical Report INL/EXT-14-32277, Rev. 4, Idaho National Laboratory (2018).

[30] Collin, B. P., AGR 3/4 Irradiation Test Final As Run Report. Technical Report INL/EXT-15-35550, Idaho National Laboratory (2015).

[31] Demkowicz, P. A., Reber, E. L., Scates, D. M., Scott, L., and Collin, B. P. (2015) First high temperature safety tests of AGR-1 TRISO fuel with the Fuel Accident Condition Simulator (FACS) furnace. *Journal of Nuclear Materials,* **464**, 320–330.

[32] Morris, R. N., Hunn, J. D., Baldwin, C. A., Montgomery, F. C., Gerczak, T. J., and Demkowicz, P. A. (2018) Initial results from safety testing of US AGR-2 irradiation test fuel. *Nuclear Engineering and Design,* **329**, 124–133 The best of HTR 2016: International Topical Meeting on High Temperature Reactor Technology.

[33] Pastore, G., Pizzocri, D., Hales, J., Novascone, S., Perez, D., Spencer, B., Williamson, R., Van Uffelen, P., Luzzi, L., et al. (2014) Modelling of transient fission gas behaviour in oxide fuel and application to the BISON code. In *Enlarged Halden Programme Group Meeting, Røros, Norway*.

[34] Laboure, V. M., Balestra, P., Ortensi, J., Hanophy, J. T., Prince, Z. M., Stewart, R. H., and Strydom, G., Multiphysics Pebble-Bed Reactor Control Rod Withdrawal Study. Technical Report INL/RPT-23-74341, Idaho National Laboratory (2023).

[35] Jaradat, M. K., Schunert, S., Gleicher, F. N., Labouré, V. M., and DeHart, M. D. (2024) Forward and inverse predictive transient models of TREAT using surrogate reactivity models. *Annals of Nuclear Energy,* **201**, 110449.

[36] Jaradat, M. K., Schunert, S., Gleicher II, F. N., and DeHart, M. D., Prediction of The TREAT Facility Power and Temperature of Sirius-2c Nuclear Propulsion Fuel Experiment. Technical Report INL/CON-24-76205, Idaho National Laboratory (2024).

[37] Idaho National Laboratory BISON: A Finite Element-Based Nuclear Fuel Performance Code. https://mooseframework.inl.gov/bison/; accessed 1-Jan-2023.

[38] Idaho National Laboratory Nuclear Data Management and Analysis System. https://ndmashome.inl.gov/; accessed 1-Jan-2024.

[39] Maki, J. T., Petti, D. A., Knudson, D. L., and Miller, G. K. (2007) The challenges associated with high burnup, high temperature and accelerated irradiation for TRISO-coated particle fuel. *Journal of Nuclear Materials,* **371**(1), 270–280 Nuclear Fuels and Structural Materials 1.

[40] Holschuh, T., Woolstenhulme, N., Baker, B., Bess, J., Davis, C., and Parry, J. (2019) Transient Reactor Test Facility Advanced Transient Shapes. *Nuclear Technology,* **205**(10), 1346–1353.

[41] Bess, J. D., Woolstenhulme, N. E., Davis, C. B., Dusanter, L. M., Folsom, C. P., Parry, J. R., Shorthill, T. H., and Zhao, H. (2019) Narrowing transient testing pulse widths to enhance LWR RIA experiment design in the TREAT facility. *Annals of Nuclear Energy,* **124**, 548–571.

[42] MacFarlane, D., Freund, G., and Boland, J., Hazards summary report on the Transient Reactor Test Facility (TREAT). Technical Report ANL-5923, Argonne National Laboratory (1958).

[43] Holschuh, T., Woolstenhulme, N., Baker, B., Bess, J., Davis, C., and Parry, J. (2019) Transient Reactor Test Facility Advanced Transient Shapes. *Nuclear Technology,* **205**(10), 1346–1353.

[44] Bess, J. D., Woolstenhulme, N. E., Davis, C. B., Dusanter, L. M., Folsom, C. P., Parry, J. R., Shorthill, T. H., and Zhao, H. (2019) Narrowing transient testing pulse widths to enhance LWR RIA experiment design in the TREAT Facility. *Annals of Nuclear Energy,* **124**, 548–571.

[45] Ortensi, J., Alberti, A., Wang, Y., DeHart, M., Gleicher, F., Schunert, S., and Palmer, T., Methodologies and Requirements for the Generation of Physics Data Inputs to MAMMOTH Transient Simulations in Support of the Transient Reactor Test Facility. Technical Report INL/EXT-15-36265, Idaho National Laboratory (2015).

[46] Leppänen, J., Pusa, M., Viitanen, T., Valtavirta, V., and Kaltiaisenaho, T. (2015) The Serpent Monte Carlo code: Status, development and applications in 2013. *Annals of Nuclear Energy,* **82**, 142–150 Joint International Conference on Supercomputing in Nuclear Applications and Monte Carlo 2013, SNA + MC 2013. Pluri- and Trans-disciplinarity, Towards New Modeling and Numerical Simulation Paradigms.